Long-Term and High-Temperature Storage of Supercritically-Processed Microparticulate Protein Powders

Michael A. Winters,[1] Pablo G. Debenedetti,[1,4] Jannette Carey,[2] H. Gerald Sparks,[3] Samir U. Sane,[3] and Todd M. Przybycien[3]

Received March 17, 1997; accepted June 26, 1997

Purpose. The long-term and high-temperature storage of dry, micron-sized particles of lysozyme, trypsin, and insulin was investigated. Subsequent to using supercritical carbon dioxide as an antisolvent to induce their precipitation from a dimethylsulfoxide solution, protein microparticles were stored in sealed containers at −25, −15, 0, 3, 20, 22, and 60°C. The purpose of this study was to investigate the suitability of supercritical antisolvent precipitation as a finishing step in protein processing.

Methods. Karl Fisher titrations were used to determine the residual moisture content of commercial and supercritically-processed protein powders. The secondary structure of the dry protein particles was determined periodically during storage using Raman spectroscopy. The proteins were also redissolved periodically in aqueous buffers and assayed spectrophotometrically for biological activity and by circular dichroism for structural conformation in solution.

Results. Amide I band Raman spectra indicate that the secondary structure of the protein particles, while perturbed from that of the solution state, remained constant in time, regardless of the storage temperature. The recoverable biological activity upon reconstitution for the supercritically-processed lysozyme and trypsin microparticles was also preserved and found to be independent of storage temperature. Far UV circular dichroism spectra support the bioactivity assays and further suggest that adverse structural changes, with potential to hinder renaturation upon redissolution, do not take place during storage.

Conclusions. The present study suggests that protein precipitation using supercritical fluids may yield particles suitable for long-term storage at ambient conditions.

KEY WORDS: supercritical fluid antisolvent; protein precipitation; secondary structure; solid state; long-term storage.

INTRODUCTION

Individual contributions to the free energy difference between native and unfolded states of a protein in solution are relatively large, on the order of 10^3 kcal/mol (e.g., intramolecular hydrogen bonds, disulfide bonds, solvent restructuring). However, the sum of these contributions yields marginal stability, ranging from −5 to −10 kcal/mol. This inherent frailty makes a protein susceptible to a variety of intramolecular and intermolecular chemical reactions capable of irreversibly perturbing its native conformation and rendering it biologically inactive (1). Such deleterious processes, including hydrolysis, covalent and noncovalent aggregation, deamidation, disulfide scrambling, oxidation, and β-elimination (2), occur in an aqueous environment (3,4). Also, microbial contamination of protein solutions during synthesis, purification, or storage may result in enzymatic degradation (5). Consequently, in order to increase their stability and usefulness as biopharmaceuticals, proteins are often formulated in the solid state with the expectation of increased shelf-life.

Final product formulation for bulk solid-state storage is most commonly accomplished via lyophilization. Recently an alternative process for the formulation of dry, microparticulate protein powders has been developed (6–8). This technique involves using a supercritical fluid antisolvent (SAS) to induce rapid protein precipitation from an organic solvent. Precipitates of model proteins exhibit minimal to intermediate losses of biological activity upon rehydration in aqueous buffers (6,8). This observation, coupled with Coulter counter analyses and SEM micrographs which indicate that protein precipitates are in the 1–5 μm size range, suggests that SAS-produced microparticles may be well-suited for long-term storage and for the development of controlled release and pulmonary aerosol drug delivery devices. In addition to its application to proteins, this technique is also attractive for the micronization and formulation of a variety of materials (see (9) for a recent review of materials and chemical processing with supercritical fluids) (10–17).

In solid-state protein formulations, because of the high effective protein concentrations, intermolecular associations and aggregation may arise and reversibly or irreversibly denature proteins (18,19). Lyophilization subjects proteins to the damaging stresses of freezing and drying (20–22); often lyophilized formulations include lyoprotectants to enhance the stability of proteins during freeze-drying (23). Supercritical fluid antisolvent processing also exposes proteins to potentially deactivating environments, including organic and supercritical nonaqueous solvents, high pressure, and shearing forces (6). Amide I band Raman and FTIR spectroscopic measurements have revealed that the most significant alteration in secondary structure during supercritical fluid-induced protein precipitation is a marked increase in β-sheet and substantial loss of α-helicity, indicative of β-sheet-mediated intermolecular interactions (7,8). Insulin, lysozyme and trypsin, when subjected to SAS processing, unfolded to various degrees. Analyses of Raman spectra for lysozyme, trypsin, and insulin precipitates revealed minimal, intermediate, and appreciable changes, respectively, in secondary structure with respect to their starting forms as commercially-lyophilized powders and to their native solution structures (8).

Current theory involving the long-term storage of dried proteins indicates that for extended stability it is preferable to store proteins in their native state (19,22). With this in mind and the knowledge that SAS processing leads to non-native solid-state conformations, the purpose of this study was to explore the long-term and high-temperature storage of lysozyme, trypsin, and insulin powders formulated using supercritical fluid antisolvent-induced precipitation. Lysozyme, trypsin, and insulin, known to be rather stable as lyophilized powders,

[1] Department of Chemical Engineering, Princeton University, Princeton, New Jersey 08544-5263.
[2] Chemistry Department, Princeton University, Princeton, New Jersey 08544-5263.
[3] Isermann Department of Chemical Engineering, Rensselaer Polytechnic Institute, Troy, New York 12180-3590.
[4] To whom correspondence should be addressed.

0724-8741/97/1000-1370$12.50/0

were the only proteins to have been SAS-processed prior to this study. Thus the storage of lysozyme, trypsin, and insulin was a logical starting point for the present study, which is the first to examine the shelf-life of protein powders generated with SAS, a relatively stringent precipitation technique.

With amide I band Raman spectroscopy, we investigated the secondary structure of the SAS-precipitated proteins stored in the solid state at temperatures of −25, −15, 0, 20, and 60°C. The reconstitution characteristics of the SAS-precipitated proteins were studied as a function of storage time and temperature (−15, 3, and 22°C) using spectrophotometric biological activity assays and circular dichroism. For comparison, commercially-lyophilized lysozyme, trypsin, and insulin powders, the starting materials in the SAS process, were stored and analyzed under identical conditions. Karl Fisher titrations were used to determine the residual moisture content of commercial and processed protein powders; this is a critical stability characteristic for solid-state formulations (2). Results for these model proteins indicate that SAS-induced structural perturbations do not hinder the capability of the solid-state proteins to recover their biological activity following storage for extended time periods.

MATERIALS AND METHODS

Chemicals

Microcrystalline egg white lysozyme (lot No. 111H7010), crystallized (3x), dialyzed, and lyophilized, was obtained from Sigma Chemical Company (St. Louis, MO). Type III bovine pancreas trypsin (lot No. 24H0070), dialyzed and lyophilized, was also purchased from Sigma. Low endotoxin bovine insulin was purchased as a lyophilized Zn powder from Sigma (lot No. 74H0084) and from Miles Inc. (Kankakee, IL; lot No. 308). Insulin from Sigma was processed to yield samples I1 and I3; Miles insulin was processed to yield sample I2. Spectrophotometric grade dimethylsulfoxide (DMSO) of 99.9% purity (lot No. 943589) was obtained from Fisher Scientific (Pittsburgh, PA). Liquid carbon dioxide (CO_2) of 99.8% purity was purchased from MG Industries (Philadelphia, PA). All chemicals were used as received, with no further purification.

Supercritical Fluid Antisolvent-Induced Precipitation of Protein Micropowders

The technique of using a supercritical fluid as an antisolvent to induce the precipitation of microparticles from an organic phase has been described elsewhere in detail (6,11,13). In brief, we dissolve the commercial protein of interest in DMSO and then spray the liquid organic solution into a continuum of co-currently flowing supercritical CO_2 (Table 1 lists the precipitation conditions, which varied between experiments). Because of the mutual solubility of CO_2 and DMSO, there is two-way mass transfer. The DMSO evaporates into the CO_2 and the supercritical fluid dissolves into the DMSO, swelling the liquid phase. Because CO_2 has low affinity for proteins, the dissolved CO_2 decreases the solvent strength of the DMSO towards the protein, causing precipitation in the form of 1 to 5 μm-sized particles. Eventually, the DMSO evaporates into the continuum CO_2 phase. The resulting CO_2-rich single fluid phase flows through a 0.5 μm pore-sized metal filter leaving the solid protein phase behind. When a sufficient amount of protein (typically 100 to 400 mg) has precipitated, pure CO_2 is flowed over the protein phase to remove any residual DMSO. The protein particles are then collected and stored immediately following slow depressurization of the precipitator vessel to ambient conditions. No attempt was made to control the humidity within the precipitator vessel upon depressurizing, and consequently samples were temporarily (<10 min) exposed to moisture in the ambient air.

Storage of Commercial and Processed Protein Particles

200 mg samples of either supercritically-processed or commercial powders were each individually sealed in separate 2 mL air-tight Fisherbrand microcentrifuge tubes. Lysozyme samples analyzed with Raman spectroscopy were stored at either 60°C for 3 days or at 20, 0, or −25°C for approximately 12 months. Lysozyme samples stored at 60°C were initially stored for two months at 0°C, and those reconstituted for biological activity assays and circular dichroism studies were stored for approximately 12 months at −15, 3, or 22°C. Samples of trypsin and insulin were stored at both 60°C for 3 days and −15°C for 1.5 yr (trypsin) and 2 yr (insulin). Trypsin and insulin samples stored at 60°C were initially stored at −15°C for about 1.5 and 2 yr, respectively. At specific time intervals, microcentrifuge tubes were opened following thermal equilibration to room temperature to prevent condensation of water vapor. A solid sample (approximately 10 mg) was removed for solid-state and rehydration analyses prior to resealing microcentrifuge tubes.

Residual Moisture Content

Karl Fisher titrations were performed on a Mitsubishi Moisture Meter (model CA-06) equipped with a water vaporizer (model VA-06). Mitsubishi Moisture Meter cathode (10 mL, lot No. D94108) and anode (150 mL, lot No. E95918) solutions were used. Between 15 and 50 mg of solid sample stored as reported were delivered to the sample boat of the vaporizer, and the vaporizer oven temperature was set for 130°C. The back purge time, conditioning time, and boat cooling/sample introduction times were set for 0.5, 1.0, and 3.0 min, respectively. The background moisture rate in the N_2 stream typically leveled out between 0.09 and 0.17 μg/s. The detector sensitivity was set for 0.10 μg/s. Titrations automatically stopped after approximately 5 min when the flow rate of H_2O (μg/s) was below the sum of the initial background moisture rate and the detector sensitivity setting.

Raman Spectroscopy

Spectra were acquired with a Jobin-Yvon T-64000 spectrometer operating in the triple subtractive mode. Slit settings of 0.4, 27, and 0.4 mm gave a bandpass of nearly 8 wavenumbers. Hardware details have been previously described (8). Solid samples were pressed manually between glass slides and examined with microprobe optics with the top slide removed. Alternatively, samples were packed into Kimax melting point capillaries and examined with macroscopic collection optics in the backscattering mode. Spectra for all samples examined with macroscopic optics were acquired in sets of 16, with an incident power of approximately 5 mW at the 514.5 nm line of an Ar^+ laser, with collection times of 60 s per spectrum. Spectra

collected using microscopic optics were acquired in sets of 8 or 9, with accumulation times of 300 s per spectrum and an incident power of roughly 3 mW. Postcollection spectral processing including detector spike removal, frequency calibration, and subtractions due to aromatic and fluorescence contributions was performed as described by Yeo *et al.* (7). Secondary structure analyses were performed on processed spectra with a Raman spectral analysis software package (RSAP) (24). While structural estimates were previously shown to be independent of spectral signal-to-noise ratio (S/N) into the single-digit range, in this work S/N ranged from 10 to 328, excluding two out of 126 measured spectra, with values of 8 and 9. For trypsin and insulin samples, the root-mean-square structure fitting error (RNORM) ranged from 3.1 to 4.0%. With the exception of four of the 102 lysozyme structure estimates, RNORM values ranged from 3.1 to 4.7% (the four RNORM values not in the 3.1 to 4.7% range were 5.6, 5.9, 6.1, and 6.2%).

Lysozyme Biological Activity Assay

Details of the lysozyme activity assay are given elsewhere (8). Briefly, the enzyme solution, consisting of approximately 15 μg/mL of lysozyme dissolved in 0.068 M phosphate buffer (pH 6.6), was visibly clear. The actual concentration of soluble lysozyme was found by dividing the absorbance readings at 280 nm by an extinction coefficient of 2.6 cm^2/mg and a path-length of 1.0 cm (25). Upon adding 0.25 mL of the enzyme solution to 2.5 mL of a bacterial suspension, the decrease in absorbance was monitored at 450 nm and remained linear for 3 to 4 min. The activity was then obtained as the ratio of the initial slope of the absorbance versus time curve to the protein concentration in the assay solution. All reported percent activities are relative to the activity of the commercial lysozyme sample stored at −15°C.

Trypsin Biological Activity Assay

Details of the trypsin activity assay are given elsewhere (8). Briefly, commercial and processed trypsin samples were redissolved in 0.05 M tris-HCl (pH 7.8) to approximately 0.3 mg/mL. At this concentration, enzyme solutions were clear and contained no visible aggregates. The actual concentration of soluble trypsin was determined from absorbance readings at 281.5 nm through a 1 cm path-length cell, using an extinction coefficient of 1.4 cm^2/mg (25). The rate at which the absorbance at 253 nm increased upon adding 0.1 mL of enzyme solution to 3.0 mL of peptide substrate N,α-benzoyl-L-arginine ethyl ester hydrochloride (BAEE, lot No. 34H0409, Sigma Chemical Co.) and 0.1 mL of distilled water was measured for 2 to 3 min. The activity was given by the ratio of the initial slope of the absorbance versus time curve to the protein concentration in the assay solution. All reported percent activities are relative to the activity of the commercial trypsin sample stored at −15°C.

Circular Dichroism Spectroscopy

Far UV circular dichroism (CD) spectra were acquired with an Aviv Associates model 60 DS spectropolarimeter (Lakewood, NJ) operating in wavelength scan mode. Solution samples were drawn into a 0.2 cm path-length quartz cuvette, and their temperature was maintained at 22.0°C with a Peltier thermal-controlled cell holder. Spectra were obtained from 240.0 to 200.0 nm, with an increment of 0.25 nm, an average integration time of 1.0 s, and a 1.5 nm bandwidth setting. Spectra for all samples were acquired in sets of 8. Lysozyme samples were redissolved in 0.2 M NaCl, with pH adjusted to 6.70 using dilute NaOH and HCl solutions. Solutions were briefly sonicated to ensure lysozyme dissolution and syringe filtered through a 0.1 μm nylon membrane to remove insoluble aggregates formed during SAS processing. The concentration of lysozyme was determined spectrophotometrically by measuring the absorbance at 280 nm through a 1.0 cm path-length cuvette and by using an extinction coefficient of 2.6 cm^2/mg (25). Spectra of the 0.2 M NaCl were subtracted from spectra of the lysozyme solution samples. The circular dichroism results are reported in terms of [θ], the mean residue ellipticity, with units deg·cm^2/dmol (26). The mean residue weight was taken as 111 g/mol, found by dividing the molecular weight of lysozyme (14388 g/mol) (25) by the number (129) of amino acid residues in lysozyme (27).

RESULTS AND DISCUSSION

Assessing the long-term stability of insulin, trypsin, and lysozyme in the solid state involves: (1) generating dry protein powders using supercritical antisolvent precipitation, (2) storing SAS-processed powders and, for comparison, commercially-lyophilized forms, (3) measuring secondary structure content as a function of storage time, (4) reconstituting powders into aqueous solutions as a function of time to enable the measurement of recovered biological activity and ability to refold to native conformation, and (5) comparing results of SAS-processed and lyophilized forms. Steps (1) to (4) have been described above. The experimental operating conditions used in the supercritical fluid antisolvent (SAS) production of insulin, trypsin, and lysozyme microparticles are listed in Table I. The SAS-processed powders (I1–I5, T1–T6, and L1–L3) were each precipitated in distinct experiments.

Also indicted in Table I are the residual water contents of the commercial and processed powders as determined by Karl Fisher titrations. Measurements were made on samples stored as reported. The moisture content was not determined for trypsin samples T1, T2, and T3. The residual water content of SAS-processed insulin samples is lower than commercially-lyophilized insulin regardless of the operating conditions during precipitation. Conversely, SAS-processed trypsin and lysozyme samples (with the exception of L2) are less dehydrated than their respective starting forms, suggesting that residual moisture upon SAS processing is protein dependent.

Samples were exposed to ambient air for roughly 10 min during collection, as the humidity of the precipitator vessel was not controlled following depressurization. Thus the measured moisture contents represent the water transferred to or from the protein samples during SAS processing and that added during collection. Further experiments under controlled ambient humidity and DMSO water content will be conducted.

Long-Term Conformational Stability of Microparticulate Protein Powders

Aromatic and fluorescence background-subtracted amide I band Raman spectra for various solid samples of insulin,

Table I. Experimental Conditions During SAS Precipitation and Residual Moisture Content in Protein Powders

Form[a]	Temp[b] (°C)	Pressure[c] (bar)	Conc[d] (mg/mL)	Flow rate[e] (mL/min)	Flow rate[f] (SLPM)	Moisture[g] (wt %)
			Insulin			
Lyophilized	—	—	—	—	—	3.26 ± 0.43
SAS ppt I1	35	91	9.2	1.7	13	2.82 ± 0.06
SAS ppt I2	37	91	4.0	1.2	13	2.97 ± 0.04
SAS ppt I3	46	142	4.2	1.7	9	2.69 ± 0.14
SAS ppt I4	43	91	4.0	0.9	26	2.81 ± 0.22
SAS ppt I5	41	94	5.3	1.9	11	1.85 ± 0.22
			Trypsin			
Lyophilized	—	—	—	—	—	4.20 ± 0.49
SAS ppt T1	38	91	3.8	2.1	11	—
SAS ppt T2	47	129	3.8	1.7	10	—
SAS ppt T3	28	136	3.8	2.0	10	—
SAS ppt T4	35	115	4.0	1.4	13	6.75 ± 0.21
SAS ppt T5	40	115	4.0	0.9	10	7.29 ± 0.15
SAS ppt T6	40	173	4.2	1.8	8	5.41 ± 0.98
			Lysozyme			
Lyophilized	—	—	—	—	—	2.92 ± 0.34
SAS ppt L1	36	91	6.8	1.7	15	7.38
SAS ppt L2	34	92	8.1	1.1	11	2.51
SAS ppt L3	41	92	7.7	1.7	17	3.92

[a] Lyophilized: commercially-lyophilized powder, as received from Miles (insulin) and Sigma (trypsin, lysozyme). SAS ppt: supercritical antisolvent-processed protein precipitate.
[b,c] Operating temperature and pressure during supercritical fluid antisolvent-induced precipitation of protein.
[d] Protein concentration in neat DMSO.
[e] Flow rate of the organic protein solution sprayed into supercritical CO_2.
[f] Supercritical fluid flow rate measured in standard liters per minute (L/min at 273.15 K and 1 atm).
[g] Residual water content of stored protein powders as measured by Karl Fisher titrations. Measurements were not made for SAS ppt T1, T2, and T3.

trypsin, lysozyme are shown in Figure 1 (A and B correspond to long-term and elevated temperature storage, respectively). Raman spectroscopy enables the measurement of vibrations in amide bonds of the protein backbone. These vibrations, primarily due to carbonyl group stretching and amide group wagging, give rise to the amide I spectral band from 1640 to 1690 cm^{-1}, and are sensitive to the conformation of the protein backbone and are thus indicative of the secondary structure of the protein molecule. The intent of Figure 1A is to illustrate that following approximately 2 (insulin) and 1.5 (trypsin) years of storage at −15°C the secondary structure of SAS-processed powders is unchanged.

Each processed insulin and trypsin powder was precipitated using operating conditions listed in Table I. The observation that the amide I band spectrum of processed insulin and trypsin powders does not change with storage time suggests that experimental conditions during SAS-induced protein precipitation do not influence the shelf-life or long-term stability of the protein micropowders. This assumption is valid for the SAS operating conditions listed in Table I, which range from 35 to 46°C, 91 to 142 bar for insulin samples and from 28 to 47°C, 91 to 136 bar for trypsin samples.

Curves g & n represent, respectively, the spectra of commercial insulin and trypsin powder, the starting materials before SAS processing. These commercial samples were stored at −15°C in the same manner as the SAS-processed samples. Upon close inspection, it can be seen that the position of the amide I band maximum in curves a & b, c & d, and e & f has shifted roughly +15 cm^{-1} relative to the commercial starting insulin. Likewise, the amide I band maximum in curves h & i, j & k, and l & m has shifted +5 cm^{-1} relative to commercial trypsin. These shifts are suggestive of increased β-sheet content with concomitant loss of α-helicity, a seemingly general event accompanying the SAS processing of proteins (7,8). These perturbations, analogous to findings for salt-induced protein precipitation (28), may be interpreted in terms of increased β-sheet-mediated protein-protein interactions within the amorphous SAS precipitates.

The secondary structure content of lysozyme powders (L1) stored at −25, 0, and 20°C was measured as a function of time using Raman spectroscopy. Secondary structure estimates from amide I band Raman spectra of commercial and SAS-processed lysozyme powders are shown in Figure 2. The symbols in Figure 2A, B, and C represent the total helix, total sheet, and turns plus unordered structural contents of the protein powders at specific storage times and temperatures. The open symbols correspond to the as-received, commercially-lyophilized lysozyme, and the filled symbols are for the SAS-processed lysozyme. For each lysozyme powder, regardless of the storage temperature, the secondary structure is unchanged with time. The fluctuations in the data points, notably those that represent the total helix and sheet contents of SAS-processed lysozyme samples, are within the error associated with the Raman structural analysis.

Table II displays the RSAP structural estimates, S/N ratios, and RNORM values for the insulin and trypsin spectra illus-

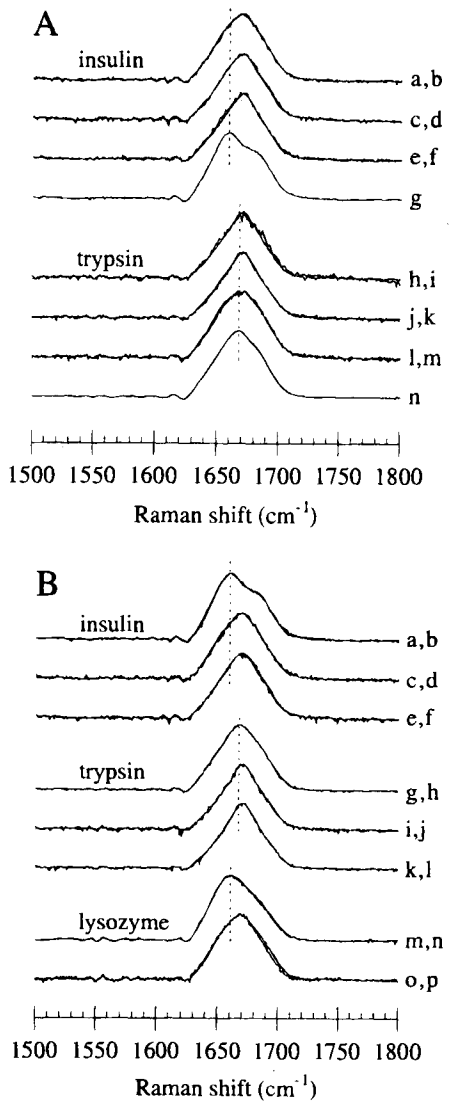

Fig. 1. (**A**) Aromatic and fluorescence-subtracted amide I band Raman spectra of solid-state insulin and trypsin samples stored at −15°C: (a, c, e) I1, I2, and I3 immediately after SAS-processing, (b, d, f) I1, I2, and I3 following 690 days of storage, (g) commercially-lyophilized insulin powder, (h, j, l) T1, T2, and T3 immediately after SAS-processing, (i, k, m) T1, T2, and T3 following 450 days of storage, and (n) commercially-lyophilized trypsin powder. Noise of trypsin spectra (h), (j), and (l) due to collection at lower S/N [S/N for spectra (h), (i), (j), (k), (l), (m): 33, 132, 67, 286, 51, 165]. (**B**) Aromatic and fluorescence-subtracted amide I band Raman spectra of solid-state insulin, trypsin, and lysozyme samples stored at an elevated temperature: (a, c, e) commercially-lyophilized insulin, I1, and I2 prior to storage at 60°C, (b, d, f) commercially-lyophilized insulin, I1, and I2 following 72 hours of storage at 60°C, (g, i, k) commercially-lyophilized trypsin, T1, and T2 prior to storage at 60°C, (h, j, l) commercially-lyophilized trypsin, T1, and T2 following 72 hours of storage at 60°C, (m, o) commercially-lyophilized lysozyme and L1 prior to storage at 60°C, and (n, p) commercially-lyophilized lysozyme and L1 following 72 hours of storage at 60°C. Dotted lines at 1659, 1668, and 1661 cm^{-1} represent, respectively, the peak positions of the amide I band in spectra of lyophilized insulin, trypsin, and lysozyme, the starting materials.

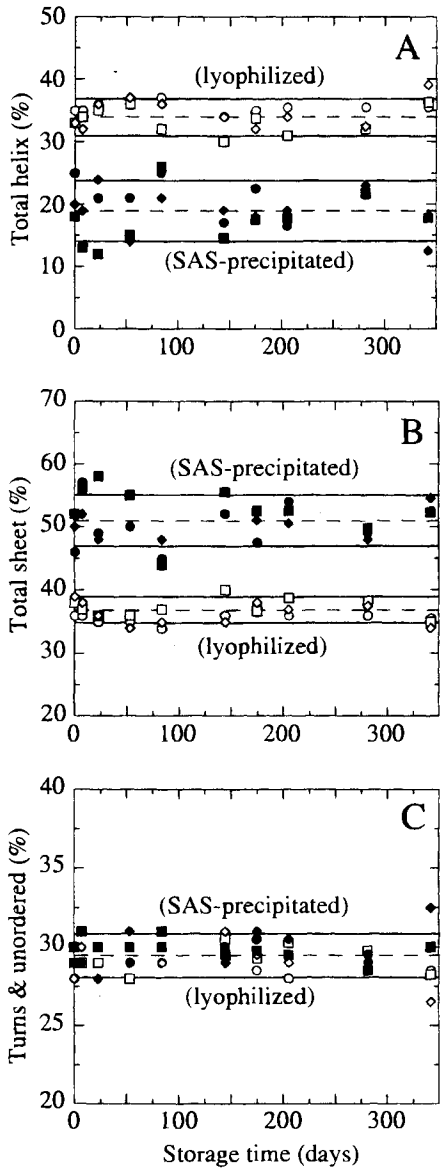

Fig. 2. Estimates of secondary structure content of stored SAS-processed and commercially-lyophilized lysozyme powders as measured by Raman spectroscopy: (**A**) % total helix, (**B**) % total sheet, and (**C**) % turns & unordered. (○, □, ◇) and (●, ■, ◆) denote, respectively, commercial and SAS-processed lysozyme stored at −25, 0, and 20°C. For visual guidance, dashed and solid lines represent the mean and ± one standard deviation of RSAP estimates, respectively.

trated in Figure 1A. Note the striking similarity of structure estimates before and following long-term storage. This further supports the notion that the secondary structure of SAS-processed insulin and trypsin remain constant with time when stored at −15°C, regardless of operating conditions during supercritical fluid-induced protein precipitation.

Also listed in Table II are structural estimates, S/Ns, and RNORMs for spectra of lysozyme samples stored at −25, 0, and 20°C, calculated by averaging the measurements collected during the storage period (Figure 2). For each storage time-averaged RSAP structural estimate, (±) values corresponding to one standard deviation are listed in Table II. The magnitudes of the standard deviations, well within the root-mean-square

Table II. Secondary Structure Estimates of Long-Term Stored Protein Powders by Amide I Band Raman Spectroscopy

Form[a]	Storage time, temp[b] (yr, °C)	H_T[c] (%)	S_T[d] (%)	U[e] (%)	S/N[f]	RNORM[g] (%)
			Insulin			
SAS ppt I1	0, −15	17	53	30	84	3
SAS ppt I1	2, −15	17	53	29	91	3
SAS ppt I2	0, −15	12	57	31	69	3
SAS ppt I2	2, −15	13	56	31	67	3
SAS ppt I3	0, −15	11	59	30	78	3
SAS ppt I3	2, −15	9	62	29	120	3
			Trypsin			
SAS ppt T1	0, −15	9	63	29	33	4
SAS ppt T1	1.5, −15	7	65	28	132	3
SAS ppt T2	0, −15	6	67	27	67	4
SAS ppt T2	1.5, −15	7	65	28	286	3
SAS ppt T3	0, −15	24	49	27	51	4
SAS ppt T3	1.5, −15	21	50	28	165	4
			Lysozyme			
Lyophilized	1, −25	35 ± 1	36 ± 1	29 ± 1	156	4
Lyophilized	1, 0	33 ± 3	37 ± 2	29 ± 1	126	4
Lyophilized	1, 20	35 ± 3	36 ± 2	29 ± 1	115	4
SAS ppt L1	1, −25	20 ± 4	50 ± 4	30 ± 1	118	4
SAS ppt L1	1, 0	18 ± 5	52 ± 4	30 ± 1	85	4
SAS ppt L1	1, 20	19 ± 4	51 ± 4	30 ± 2	82	4

[a] SAS ppt: supercritical antisolvent-processed protein precipitate. Lyophilized: commercially-lyophilized powder, as received from Miles (insulin) and Sigma (trypsin, lysozyme).
[b] For insulin and trypsin samples, time in storage prior to Raman analyses. Duration of storage period of lysozyme samples.
[c] Total helix, H_T, gives ordered and disordered α-helix contributions.
[d] Total sheet, S_T, represents contributions from antiparallel and parallel β-sheet.
[e] Undefined structure, U, gives β-reverse turn and random coil contents.
[f] Amide I band signal-to-noise ratio.
[g] RNORM: norm of the residual structure fit vector.
[c–g] Structure estimates, signal-to-noise ratios, and RNORM values for lysozyme samples were computed by averaging available measurements collected during the storage for each sample. (±) numbers represent one standard deviation with respect to the average of RSAP structural estimates for each sample collected during storage the period.

fitting error, reflect the invariance of the secondary structure of commercially-lyophilized and SAS-processed proteins during storage. The displayed standard deviations, however, should be interpreted with caution as they do not take into account the error associated with spectral deconvolution.

Unlike the SAS-processed lysozyme samples of Table II which were produced in the same precipitation experiment (L1) and then stored at different temperatures (−25, 0, and 20°C), the SAS-processed insulin and trypsin samples were precipitated under different conditions and stored at an identical temperature, −15°C. The concept behind storing insulin and trypsin was not to study the effect of temperature during long-term storage (>1 yr), as was done for lysozyme. Instead, the intent was to investigate the nature of SAS processing-induced structural perturbations and to identify processing conditions which lead to structural perturbations that inhibit the protein's conformational stability during long-term storage. To this end, processing conditions during the production of insulin and trypsin samples were varied over a wide range (Table I).

The different SAS processing conditions account for differences in RSAP structural estimates between insulin samples I1, I2, and I3 in Table II. Note, however, the absence of any systematic trend. This suggests that other factors, such as water uptake during or immediately following SAS processing, may also be important. The same is true for trypsin samples T1, T2, and T3. T3 is anomalous in that of all the SAS-processed samples, it is the only one with increased helix content and decreased sheet content relative to lyophilized trypsin. Structure estimates indicate that T1 and T2 were similar in secondary structure throughout the duration of the study, whereas T3 was consistently different. The similarity of structural estimates before and after long-term storage suggests that long-term structural stability is not critically dependent on a precisely defined conformation after SAS-processing.

Conformational Stability of Protein Powders Stored at 60°C

Aromatic and fluorescence background-subtracted amide I band Raman spectra for solid samples of insulin, trypsin, and lysozyme stored at 60°C for 72 hr are shown in Figure 1B. The similarities in the position of the spectral peaks [centered at 1659, 1669, and 1661 cm^{-1} for the commercial insulin, trypsin, and lysozyme samples (curves a & b, g & h, and m & n) and at approximately 1671, 1672, and 1669 cm^{-1} for the processed insulin, trypsin, and lysozyme samples (curves c–f, i–l, and o & p)] suggest that neither the secondary structure of the commercially-lyophilized, nor that of the SAS-processed pow-

ders changed following storage at 60°C. The roughly +8 cm^{-1} shift of the amide I band peak positions in spectra of the processed lysozyme samples (curves o & p) relative to the commercial samples (curves m & n) is again indicative of increased β-sheet formation upon SAS processing.

Additional RSAP structural estimates, S/Ns, and RNORMs for spectra of Figure 1B are listed in Table III. The similarity of the structural estimates of samples before and after 60°C storage reflects the ability of these dried powders to resist conformational perturbation. Slight variations in structure for both lyophilized and processed samples are well within the root-mean-square fitting error.

Recovery of Activity Following Long-Term Storage

Results from biological activity assays are illustrated in Figure 3A. The amount of recovered activity (~85% and 90% ± 5% (29) of that for the redissolved commercial trypsin and lysozyme powders, respectively) indicates the ability of the enzyme to renature upon aqueous dissolution (as reported previously) (8). It can be seen that the amount of recoverable activity following SAS processing is maintained with time. In accordance with the previously described long-term secondary structure findings, these results indicate that the structure of the stored protein powders does not deteriorate with time. The ability of the proteins to renature upon redissolution in aqueous solution is not adversely affected by long-term storage in powder form.

The filled symbols of curve a in Figure 3A are the percent of recovered activity for redissolved lysozyme samples stored at −15, 3, and 22°C. The fact that the recovered activities are maintained over time suggests that it is possible to store lysozyme samples in their SAS-processed form at ambient temperature without structural deterioration. The open symbols of curve b are the percent of recovered activity for redissolved trypsin samples. The conclusions are the same as for lysozyme. No measurements involving the activity of long-term stored SAS-processed insulin have been made. Previous studies involving

Table III. Secondary Structure Estimates of Protein Powders Stored at 60°C by Amide I Band Raman Spectroscopy

Form[a]	Storage time[b] (hr)	H_T[c] (%)	S_T[d] (%)	U[e] (%)	S/N[f]	RNORM[g] (%)
		Insulin				
Lyophilized	0	46	28	26	112	4
Lyophilized	72	42	30	28	69	4
SAS ppt I1	0	17	53	29	91	3
SAS ppt I1	72	14	55	31	95	4
SAS ppt I2	0	13	56	31	67	3
SAS ppt I2	72	13	57	30	38	3
		Trypsin				
Lyophilized	0	15	53	32	111	4
Lyophilized	72	16	52	32	114	4
SAS ppt T1	0	6	62	32	101	3
SAS ppt T1	72	6	67	28	56	4
SAS ppt T2	0	7	65	28	96	3
SAS ppt T2	72	5	69	26	77	4
		Lysozyme				
Lyophilized	0	36	36	28	533	4
Lyophilized	72	34	37	29	130	4
SAS ppt L1	0	15	55	30	71	3
SAS ppt L1	72	13	57	30	27	4

[a] Lyophilized: commercially-lyophilized powder, as received from Miles (insulin) and Sigma (trypsin, lysozyme). SAS ppt: supercritical antisolvent-processed protein precipitate.
[b] Storage time at 60°C.
[c] Total helix, H_T, ordered and disordered α-helix.
[d] Total sheet, S_T, antiparallel and parallel β-sheet.
[e] Undefined structure, U, β-reverse turn and random coil.
[f] Amide I band signal-to-noise ratio.
[g] RNORM: norm of the residual structure fit vector.

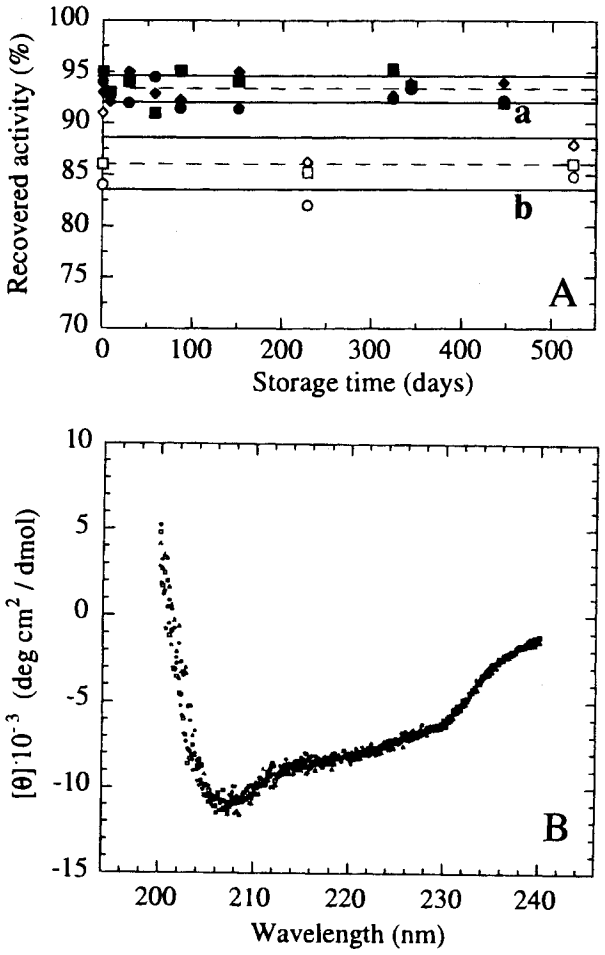

Fig. 3. (**A**) Percent of recoverable biological activity upon rehydration following SAS processing and extended storage, relative to the activity of redissolved commercial powders: (a) L1 stored at −15°C (●), 3°C (■), and 22°C (♦) following precipitation at 36°C and 91 bar; (b) T1 stored at −15°C following precipitation at 38°C and 91 bar (○), T2 stored at −15°C following precipitation at 47°C and 129 bar (□), and T3 stored at −15°C following precipitation at 28°C and 136 bar (◇). Dashed and solid lines represent, respectively, the mean and standard deviations. (**B**) Solvent-subtracted CD spectra of rehydrated lysozyme samples after 12.5 months of storage at various temperatures: (○) commercial stored at −15°C, (◇) L1 stored at 3°C, (□) L1 stored at 22°C, and (△) L1 stored at −15°C. The CD spectra superimpose without having been normalized to a common value at a longer wavelength, indicating structural similarity between all rehydrated samples.

blood glucose levels in rats, however, have shown that processed insulin's activity is indistinguishable from that of the original material, irrespective of processing conditions during precipitation (6).

Reconstitution Characteristics After Long-Term Storage

Figure 3B illustrates the CD spectra of the SAS-processed lysozyme samples stored at −15, 3, and 22°C and of the commercially-lyophilized lysozyme stored at −15°C, in each case upon redissolution in aqueous buffer following 12.5 months of storage. The spectra are in excellent agreement with previously published CD spectra for native lysozyme (26). The similarity of the spectra in Figure 3B (characterized by the minimum ellipticity $[\theta]_{207.3\ nm} = -11.3, -11.6, -11.0$, and $-10.9 \cdot 10^3$ deg·cm^2/dmol, respectively, for commercial lysozyme stored at −15°C and L1 stored at −15, 3, and 22°C) are consistent with the long-term bioactivity results and reinforce the notion that irreversible structural changes, capable of hindering the renaturing process, do not take place during storage, irrespective of the storage temperature.

As mentioned in Materials and Methods, insoluble aggregates were filtered away prior to measuring the CD spectra of processed samples. The insolubles were formed during SAS processing, and the time-invariant biological activity results suggest that the insolubles were not a consequence of moisture-induced aggregation during storage.

CONCLUSIONS

Raman structural estimates, bioassays, and CD spectra provide compelling evidence that the structure of SAS-processed lysozyme is maintained during long-term storage, regardless of the storage temperature, in the range investigated (−25 to 60°C). Likewise, Raman estimates and bioassays for SAS-processed trypsin and insulin suggest that modest structural perturbations, introduced over a wide range of operating conditions during dissolution in DMSO and SAS precipitation, do not hinder the storage potential of the dried powders. This is especially noteworthy in that previous studies have shown that insulin solutions and solid-state insulin are notoriously labile and aggregation-prone during storage (2,30,31).

Moisture-induced aggregation due to intermolecular S-S bond formation via thiol-disulfide interchange reactions is a critical problem in the storage of pharmaceutical proteins (2,32). The time-invariant secondary structural estimates and biological activities suggest that the residual moisture levels of SAS-processed insulin, trypsin, and lysozyme powders are sufficiently low to inhibit water-induced aggregation. These preliminary results warrant more investigations involving accelerated storage conditions (e.g., storage at higher temperatures and moisture levels) (2,32), tests that are sensitive to chemical deterioration (sodium dodecylsulfate-polyacrylamide gel electrophoresis, isoelectric focusing, and size exclusion chromatography) (5,23,33), and using other proteins with pharmaceutical relevance.

Contrary to other findings (19,21,22), our results suggest that the solid-state storage of non-native states does not always lead to decreased stability. With characteristics indicative of increased β-sheet-mediated intermolecular associations (7,8), SAS-processed protein powders may represent an ensemble of partially unfolded states with unusually high resistance to deterioration. More work is needed to understand the molecular basis of this stability, as well as its applicability to other proteins.

Insulin, lysozyme, and trypsin are the only proteins that had been supercritically-processed prior to this study (6–8). They are therefore the natural choice for the present study, which is the first to investigate the long-term stability of protein powders formulated via supercritical fluid-induced precipitation. However, previous work had already shown both trypsin and lysozyme to be stable in dehydrated states. To obtain noticeable inactivation, dried trypsin samples must be exposed to prolonged heating at 160°C (34). Following 1 hr of 140°C heat treatment of dry lysozyme, no inactivation was observed (35). Thus, while the present study suggests that SAS processing may be a valuable finishing step in protein processing for therapeutic applications, further studies with less resilient molecules are needed to establish the generality of this conclusion.

ACKNOWLEDGMENTS

This work was generously supported by the Air Force Office of Scientific Research (Grant F49620-93-0040 to P.G.D.) and by the National Science Foundation Career Award and Research Infrastructure Programs (Grants BES-9502184 and 9413527 to T.M.P.). The authors gratefully thank SmithKline Beecham Pharmaceuticals for assistance with the Karl Fisher titrations.

REFERENCES

1. T. E. Creighton, in *Proteins: Structures and Molecular Properties*, 2nd ed.; W. H. Freeman: New York, 1993; p 327.
2. H. R. Costantino, R. Langer, and A. M. Klibanov. *J. Pharm. Sci.* **83**:1662–1669 (1994).
3. M. C. Manning, K. Patella, and R. T. Borchardt. *Pharm. Res.* **6**:903–915 (1989).
4. A. M. Klibanov. *Advances in Applied Microbiology* **29**:1–28 1983.
5. M. W. Townsend, and P. P. DeLuca. *J. Pharm. Sci.* **79**:1083–1086 (1990).
6. S.-D. Yeo, G.-B. Lim, P. G. Debenedetti, and H. Bernstein. *Biotechnol. Bioeng.* **41**:341–346 (1993).
7. S.-D. Yeo, P. G. Debenedetti, S. Patro, and T. M. Przybycien. *J. Pharm. Sci.* **83**:1651–1656 (1994).
8. M. A. Winters, B. L. Knutson, P. G. Debenedetti, H. G. Sparks, T. M. Przybycien, C. L. Stevenson, and S. J. Prestrelski. *J. Pharm. Sci.* **85**:586–594 (1996).
9. C. A. Eckert, B. L. Knutson, and P. G. Debenedetti. *Nature*, **383**:313–318 (1996).
10. D. J. Dixon, K. P. Johnston, and R. A. Bodmeir. *AIChE J.* **39**:127–139 (1993).
11. D. J. Dixon, and K. P. Johnston. *J. Appl. Polym. Sci.* **50**:1929–1942 (1993).
12. S.-D. Yeo, P. G. Debenedetti, M. Radosz, and H.-W. Schmidt. *Macromolecules* **26**:6207–6210 (1993).
13. T. W. Randolph, A. D. Randolph, M. Mebes, and S. Yeung. *Biotechnol. Bioeng.* **9**:429–435 (1993).
14. S.-D. Yeo, P. G. Debenedetti, M. Radosz, R. Giesa, and H.-W. Schmidt. *Macromolecules* **28**:1316–1317 (1995).
15. G. Luna-Bárcenas, S. K. Kanakia, I. C. Sanchez, and K. P. Johnston. *Polymer* **36**:3173–3182 (1995).
16. W. J. Schmitt, M. C. Salada, G. C. Shook, and S. M. Speaker III. *AIChE J.* **41**:2476–2486 (1995).
17. R. Bodmeir, H. Wang, D. J. Dixon, S. Mawson, and K. P. Johnston. *Pharm. Res.* **12**:1211–1217 (1995).
18. M. J. Pikal. *Biopharm* **3**:18–27 (1990).
19. A. Dong, S. J. Prestrelski, S. D. Allison, and J. F. Carpenter. *J. Pharm. Sci.* **84**:415–424 (1995).
20. H. R. Constantino, K. Griebenow, P. Mishra, R. Langer, and A. M. Klibanov. *Biochim. Biophys. Acta* **1253**:69–74 (1995).

21. S. J. Prestrelski, N. Tedeschi, T. Arakawa, and J. F. Carpenter. *Biophys. J.* **65**:661–671 (1993).
22. B. S. Kendrick, A. Dong, S. D. Allison, M. Manning, and J. F. Carpenter. *J. Pharm. Sci.* **85**:155–158 (1996).
23. T. Arakawa, S. J. Prestrelski, W. C. Kenney, and J. F. Carpenter. *Advanced Drug Delivery Reviews* **10**:1–28 (1993).
24. T. M. Przybycien, and J. E. Bailey. *Biochim. Biophys. Acta* **995**:231–245 (1989).
25. L. A. Decker, Ed. *Worthington Enzyme Manual: Enzymes, Enzyme Reagents, Related Biochemicals*; Worthington Biochemical Corp.: Freehold, NJ, 1977; pp 185–188, 221–224.
26. N. Greenfield, G. D. Fasman. *Biochem.* **8**:4108–4116 (1969).
27. D. C. Phillips. *Proc. N. A. S.* **57**:484–495 (1967).
28. T. M. Przybycien, and J. E. Bailey. *Biochim. Biophys. Acta* **1076**:103–111 (1991).
29. D. Z. Frankel, Protein Purification with Compressed Carbon Dioxide, B.S. Thesis, Princeton University, 1997.
30. V. Sluzky, J. A. Tamada, A. M. Klibanov, and R. Langer. *Proc. Natl. Acad. Sci. USA* **88**:9377–9381 (1991).
31. V. Sluzky, A. M. Klibanov, and R. Langer. *Biotech. Bioeng.* **40**:895–903 (1992).
32. W. R. Liu, R. Langer, and A. M. Klibanov. *Biotechnol. Bioeng.* **37**:177–184 (1991).
33. M. W. Townsend, and P. P. DeLuca. *J. Pharm. Sci.* **80**:63–66 (1991).
34. P. F. Mullaney. *Nature* **210**:953 (1966).
35. W. Goldbach, and R. Herzog. *Nahrung* **11**:145–147 (1967).